IEEE Photonics Journal
An IEEE Photonics Society Publication

Open Access

Dimming Control Scheme With High Power and Spectrum Efficiency for Visible Light Communications

Volume 9, Number 1, February 2017

Fang Yang, ***Senior Member, IEEE***
Junnan Gao

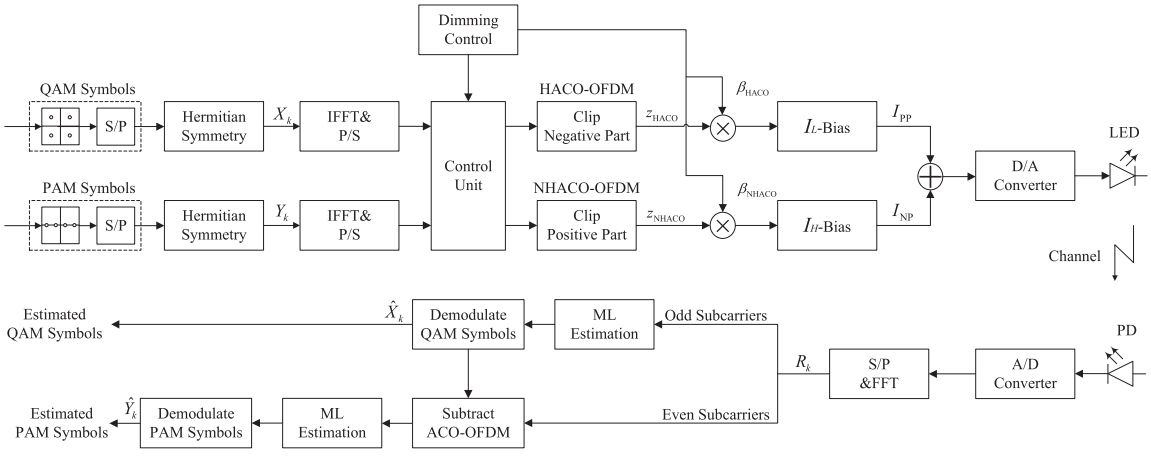

DOI: 10.1109/JPHOT.2017.2658025
1943-0655 © 2017 IEEE

IEEE photonics SOCIETY

IEEE

Dimming Control Scheme With High Power and Spectrum Efficiency for Visible Light Communications

Fang Yang, *Senior Member, IEEE*, and Junnan Gao

Research Institute of Information Technology, Tsinghua National Laboratory for Information Science and Technology (TNList), Tsinghua University, Beijing 100084, China

DOI:10.1109/JPHOT.2017.2658025

Manuscript received December 30, 2016; revised January 20, 2017; accepted January 22, 2017. Date of publication January 24, 2017; date of current version February 21, 2017. This work was supported in part by the National Natural Science Foundation of China under Grant 61401248, in part by the New Generation Broadband Wireless Mobile Communication Network of the National Science and Technology Major Projects under Grant 2015ZX03002008, in part by the Tsinghua University Initiative Scientific Research Program under Grant 2014Z06098, and in part by the Young Elite Scientist Sponsorship Program by CAST. Corresponding author: Fang Yang (e-mail: fangyang@tsinghua.edu.cn).

Abstract: In this paper, in order to accommodate dimming demands for illumination, which is an essential requirement for visible light communication (VLC), a dimming control scheme with high power and spectrum efficiency is proposed. In the proposed method, a negative hybrid asymmetrically clipped optical orthogonal frequency division multiplexing (NHACO-OFDM) is first investigated and then combined with HACO-OFDM signal for multiplexed transmission. By adjusting the proportion of these two signals, the novel dimming control scheme can be achieved. Simulation results conducted that the proposed scheme can support optical wireless communication with higher power and spectrum efficiency and carry out the dimming control with broad dimming range for illumination, compared with conventional counterparts under various illumination conditions.

Index Terms: Orthogonal frequency division multiplexing (OFDM), hybrid asymmetrically clipped optical OFDM (HACO-OFDM), dimming control, visible light communication (VLC).

1. Introduction

Due to the prompt development of the light-diode (LED), visible light communication (VLC), which makes use of the outstanding modulation capability of LED for optical wireless communication, as well as lighting, has been emerging as a promising technology for future wireless communications [1], [2]. Capable of simultaneously supporting communication and illumination, VLC has distinct advantages such as huge bandwidth, inherent security, no health concerns, and low cost [3]. Recently, the orthogonal frequency division multiplexing (OFDM) and its derivative techniques, such as direct current biased optical OFDM (DCO-OFDM) [4], asymmetrically clipped optical OFDM (ACO-OFDM) [5], pulse-amplitude-modulated discrete multitone (PAM-DMT) [6], hybrid ACO-OFDM (HACO-OFDM) [7], and layered ACO-OFDM [8] as well, have been widely adopted in VLC systems for transmission with high data rate and high spectrum efficiency.

For VLC systems, communication capability with illumination should be taken into consideration to accommodate different lighting demands and power requirements [9], where achieving efficient dimming control has an adverse effect on communication. For single carrier modulations, the

pulse-position modulation (PPM) achieves the dimming control by varying the pulse intensity [10], while the on-off keying (OOK) changes the duty cycle of pulse width modulation (PWM) to support different dimming requirements [11]. Furthermore, some coding schemes have been proposed to prevent performance degradation caused by dimming operation [12], [13]. For OFDM-based VLC systems, some dimming control schemes have been investigated. For DCO-OFDM system, the dimming control is performed by just adjusting the DC bias to achieve different average amplitudes. However, when the dimming level is very high or low, the restricted dynamic range of the transmitted signal will result in performance deterioration to DCO-OFDM system [14]. Therefore, an enhanced DCO-OFDM system is proposed to address the problem by introducing a piecewise function [15]. Based on the ACO-OFDM, reverse polarity optical-OFDM (RPO-OFDM) is investigated in [16], where the PWM signal is combined with the original ACO-OFDM to support both illumination and communication within the limits of the whole dynamic range. Nevertheless, the receiver should detect the PWM signal firstly and subsequently decode the ACO-OFDM signal. Moreover, a novel hybrid scheme by combining different layers of ACO-OFDM signals is proposed to improve the spectrum efficiency by up to two times compared to the existing counterparts [8]. In [17], an asymmetrical hybrid optical OFDM (AHO-OFDM) system, where adopting the ACO-OFDM modulation for odd sub-carriers and employing the reverse PAM-DMT scheme in even subcarriers are simultaneously merged, is investigated to support various dimming targets by a DC bias instead of PWM signal. However, the scaling factors of both the ACO-OFDM and PAM-DMT signals depend on the dimming level, which results that the decode process is sensitive to the DC bias.

In this paper, a negative HACO-OFDM (NHACO-OFDM) is firstly introduced, where the positive signal is clipped in the time domain, to leave the negative excursions unchanged. The resulting signal is added to a substantial bias so that the whole signal is still positive and the dynamic range can also be fully exploited, with a mean value below the bias level. In the proposed dimming control scheme, this NHACO-OFDM signal is used when a high illumination level is desired, while the conventional HACO-OFDM is adopted for a low illumination level as it has a lower mean value. For intermediate levels, an algebraic sum of these two signals is mixed with proper proportion. Due to the fully exploitation of the whole subcarriers in both HACO-OFDM and NHACO-OFDM signal, high spectrum efficiency can be achieved. Moreover, since both the HACO-OFDM and NHACO-OFDM signals with DC bias occupy the whole dynamic range of the LED, high power efficiency can be guaranteed compared with the conventional counterparts. Simulations verified that the proposed dimming control method can be utilized in optical wireless communication with high power and spectrum efficiency, wide dimming range, and simple receiver architecture.

The rest of this paper is organized as follows. In Section 2, the system model of optical OFDM systems is described, and the novel NHACO-OFDM approach is also introduced with the analysis of its probability distribution function (PDF). The proposed dimming control scheme is presented in Section 3. The simulation results of the system performance are presented compared with existing methods in Section 4. Finally, the conclusions are drawn in Section 5.

2. System Model

2.1 HACO-OFDM

Due to the intensity modulation and direct detection (IM/DD) for optical wireless communication, the transmitted signals have to be non-negative and real-valued. Therefore, the Hermitian symmetry is usually adopted for the whole OFDM subcarriers with size of N, excluding the 0-th and $N/2$-th subcarriers are set to zeros, to ensure that the transmitted signal is real number in the time domain. Meanwhile, in order to guarantee that the time-domain signal is non-negative, several modulation schemes, such as DCO-OFDM, ACO-ODFM, PAM-DMT, and HACO-OFDM, have been proposed.

For ACO-OFDM, the quadrature amplitude modulation (QAM) is employed just in the odd subcarriers as $\mathbf{X} = [0, X_1, 0, X_3, \cdots, X_{N/2-1}, 0, X^*_{N/2-1}, \cdots, 0, X^*_1]$. Then, the negative part of the

time-domain signal x_n is clipped to generate a unipolar signal and given by

$$x_{\mathrm{ACO},n} = \lfloor x_n \rfloor_c = \begin{cases} x_n, & x_n \geq 0 \\ 0, & x_n < 0. \end{cases} \tag{1}$$

The clipping distortion does not interfere on the original transmitted signal. Hence, the frequency-domain signal can be presented as

$$X_{\mathrm{ACO},k} = \frac{X_k}{2}, \quad \text{if } k \text{ is odd.} \tag{2}$$

For PAM-DMT, the PAM is adopted only for the imaginary part Y_k of each subcarrier, where Y_k is a real number with PAM modulation as $\mathbf{Y} = j\,[0, Y_1, Y_2, \cdots, Y_{N/2-1}, 0, Y^*_{N/2-1}, \cdots, Y^*_1]$, where $j = \sqrt{-1}$. Similar to the ACO-OFDM, the clipping can be directly applied in the PAM-DMT signal y_n to achieve the non-negative part as $y_{\mathrm{PAM},n} = \lfloor y_n \rfloor_c$ in the same manner. Moreover, the clipping distortion is only imposed on the real part of each subcarrier, therefore the frequency-domain signal without any information loss can also be represented as

$$Y_{\mathrm{PAM},k} = \frac{Y_k}{2}, \quad \text{if } k \text{ is odd.} \tag{3}$$

In HACO-OFDM, the time-domain ACO-OFDM and PAM-DMT signals are directly added for simultaneous transmission, where odd subcarriers adopt the ACO-OFDM modulation and even subcarriers employ PAM-DMT scheme. The combined time-domain signal of HACO-OFDM is represented as

$$z_{\mathrm{HACO},n} = x_{\mathrm{ACO},n} + y_{\mathrm{PAM},n}. \tag{4}$$

At the receiver, ignoring the influence of channel and noise for simplicity, the received signal $r_n = z_{\mathrm{HACO},n}$ in the frequency domain can be obtained by fast Fourier transform (FFT), and is given by

$$R_k = \frac{1}{N} \sum_{n=0}^{N-1} r_n \exp\left(\frac{-j2\pi kn}{N}\right), \quad 0 \leq k < N. \tag{5}$$

Due to the PAM-DMT modulation just using even subcarriers, the clipping distortion only impacts on the real part of the even subcarriers according to literature [7]. Hence, the clipping distortions for both ACO-OFDM and PAM-DMT only affect on the even subcarriers. Therefore, the odd subcarriers of ACO-OFDM could be firstly demodulated to avoid mutual interference as

$$\hat{X}_k = 2R_k, \quad \text{if } k \text{ is odd.} \tag{6}$$

The estimation of the transmitted ACO-OFDM signal $\hat{x}_{\mathrm{ACO},n}$ in the time domain could be achieved by $\hat{X}_k$. Then, the clipped frequency-domain signal $\hat{X}_{\mathrm{ACO},k}$ can be acquired. After subtracting $\hat{X}_{\mathrm{ACO},k}$ from the received symbols on the even subcarriers, the PAM-DMT signal in the frequency domain could be obtained as

$$\hat{Y}_k = 2 \cdot \mathrm{imag}(R_k - \hat{X}_{\mathrm{ACO},k}), \quad \text{if } k \text{ is even.} \tag{7}$$

2.2 Negative HACO-OFDM

In order to achieve dimming control, NHACO-OFDM is firstly introduced, where the time-domain positive signal is clipped while the negative counterpart is remained. For the NHACO-OFDM, the data pattern consists of the frequency-domain ACO-OFDM signal **X** and PAM-DMT signal **Y** is the same as that of the HACO-OFDM. However, following the IFFT operation, an opposite clipping distortion is imposed on the unclipped signal compared with conventional HACO-OFDM, the

time-domain negative ACO-OFDM and PAM-DMT signals are represented as

$$x_{\mathrm{NACO},n} = \lceil x_n \rceil_c = \begin{cases} 0, & x_n > 0 \\ x_n, & x_n \leq 0. \end{cases} \tag{8}$$

$$y_{\mathrm{NPAM},n} = \lceil y_n \rceil_c = \begin{cases} 0, & y_n > 0 \\ y_n, & y_n \leq 0. \end{cases} \tag{9}$$

where the operator $\lceil \cdot \rceil_c$ represents the opposite clipping distortion. Therefore, the time-domain NHACO-OFDM signal can be represented as

$$z_{\mathrm{NHACO},n} = x_{\mathrm{NACO},n} + y_{\mathrm{NPAM},n}. \tag{10}$$

Through the different clipping procedures, the unclipped ACO-OFDM signal x_n in the time domain is divided into two unipolar signals $x_{\mathrm{ACO},n}$ and $x_{\mathrm{NACO},n}$. As a consequence, the original signal can be combined with these two kinds of signals in the frequency domain:

$$X_k = X_{\mathrm{ACO},k} + X_{\mathrm{NACO},k}. \tag{11}$$

According to (2) and (11), it is obvious that the frequency-domain signal of NACO-OFDM is the same as that of the conventional ACO-OFDM signal and is given by

$$X_{\mathrm{NACO},k} = X_k/2, \quad \text{if } k \text{ is odd.} \tag{12}$$

Therefore, for NHACO-OFDM system at the receiver, the NACO-OFDM signal can be detected as ACO-OFDM in the HACO-OFDM scheme. Similarly, the negative PAM-DMT signals $Y_{\mathrm{NPAM},k} = Y_k/2$ can be estimated in the same way, which is one of the crucial contributions of this paper.

2.3 PDF OF HACO-OFDM and NHACO-OFDM

Based on the central limit theorem, both the ACO-OFDM and PAM-DMT signals in the time domain follow the Gaussian distribution with zero means [18]. After the asymmetrical clipping procedure, the PDF of the clipped signal obey a clipped Gaussian distribution and can be mathematically represented as

$$f_{x_{\mathrm{ACO}}}(x_{\mathrm{ACO},n}) = \begin{cases} \frac{1}{2}, & x_{\mathrm{ACO},n} = 0 \\ \frac{1}{\sqrt{2\pi}\sigma_{\mathrm{ACO}}} \exp\left(-\frac{{x_{\mathrm{ACO},n}}^2}{2\sigma_{\mathrm{ACO}}^2}\right), & x_{\mathrm{ACO},n} > 0, \end{cases} \tag{13}$$

where σ_{ACO} is the root mean square (RMS) of the unclipped ACO-OFDM signal with the expectation calculating as $E(x_{\mathrm{ACO}}) = \sigma_{\mathrm{ACO}}/\sqrt{2\pi}$. Similar to the ACO-OFDM, the distribution function of time-domain PAM-DMT signal $f_{y_{\mathrm{PAM}}}(y_{\mathrm{PAM},n})$ is the same as that of the ACO-OFDM, and the expectation is likewise given by $E(y_{\mathrm{PAM}}) = \sigma_{\mathrm{PAM}}/\sqrt{2\pi}$.

From (4), the PDF of the intensity modulated signal $z_{\mathrm{HACO},n}$ with unipolar property can be calculated as the convolution result between the ACO-OFDM and PAM-DMT and is given by

$$\begin{aligned} f_{z_{\mathrm{HACO}}}(z) &= f_{x_{\mathrm{ACO}}}(x_{\mathrm{ACO},n}) \otimes f_{y_{\mathrm{PAM}}}(y_{\mathrm{PAM},n}) \\ &= \frac{1}{2\pi\sigma_{\mathrm{ACO}}\sigma_{\mathrm{PAM}}} \int_0^z \left(\exp\left(\frac{-l^2}{2\sigma_{\mathrm{ACO}}^2}\right) \exp\left(\frac{-(z-l)^2}{2\sigma_{\mathrm{PAM}}^2}\right) \right) dl \\ &\quad + \frac{0.5}{\sqrt{2\pi}} \left(\frac{1}{\sigma_{\mathrm{ACO}}} \exp\left(\frac{-z^2}{2\sigma_{\mathrm{ACO}}^2}\right) + \frac{1}{\sigma_{\mathrm{PAM}}} \exp\left(\frac{-z^2}{2\sigma_{\mathrm{PAM}}^2}\right) \right) u(z) + 0.25\delta(z) \\ &= \frac{1}{2\sqrt{2\pi(\sigma_{\mathrm{ACO}}^2 + \sigma_{\mathrm{PAM}}^2)}} \exp\left(-\frac{z^2}{2(\sigma_{\mathrm{ACO}}^2 + \sigma_{\mathrm{PAM}}^2)}\right) \end{aligned}$$

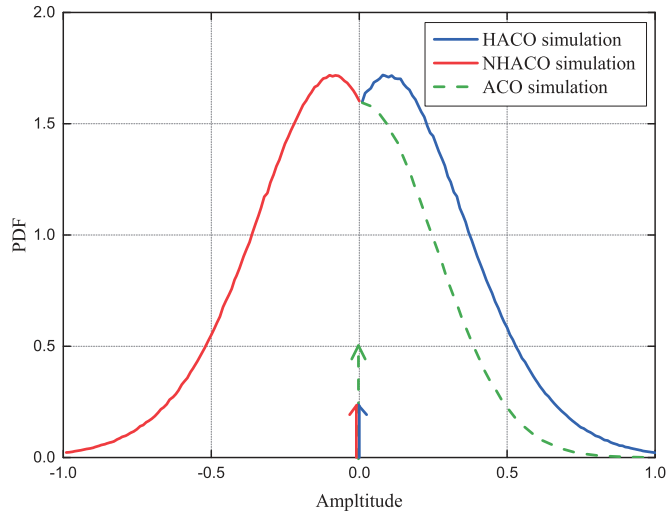

Fig. 1. PDF comparisons of ACO-OFDM, HACO-OFDM, and NHACO-OFDM.

$$\times \left[\text{erfc}\left(-\frac{\sigma_{\text{ACO}} z}{\sigma_{\text{PAM}}\sqrt{2(\sigma_{\text{ACO}}^2+\sigma_{\text{PAM}}^2)}} \right) - \text{erfc}\left(\frac{\sigma_{\text{PAM}} z}{\sigma_{\text{ACO}}\sqrt{2(\sigma_{\text{ACO}}^2+\sigma_{\text{PAM}}^2)}} \right) \right] + \frac{0.5}{\sqrt{2\pi}} \left(\frac{1}{\sigma_{\text{ACO}}} \exp\left(\frac{-z^2}{2\sigma_{\text{ACO}}^2} \right) + \frac{1}{\sigma_{\text{PAM}}} \exp\left(\frac{-z^2}{2\sigma_{\text{PAM}}^2} \right) \right) u(z) + 0.25\delta(z) \tag{14}$$

where $\otimes$, $u(z)$, $\delta(z)$, and erfc$(\cdot)$ denote the convolutional operator, unit-step function, Dirac delta function, and the complementary error function, respectively. The RMS of HACO-OFDM signal is $(\sigma_{\text{ACO}}+\sigma_{\text{PAM}})/\sqrt{2\pi}$ by calculation. Similarly, the NHACO-OFDM signal has the same RMS with the HACO-OFDM signal, while the PDF is symmetrical and can be represented as

$$f_{z_{\text{NHACO}}}(z) = f_{z_{\text{HACO}}}(-z). \tag{15}$$

Fig. 1 shows the simulated PDFs of the HACO-OFDM and NHACO-OFDM with $\sigma_{\text{ACO}} = \sigma_{\text{PAM}} = 0.25$, while the conventional ACO-OFDM is also depicted as a benchmark. It can be seen that the PDFs of HACO-OFDM and NHACO-OFDM are symmetrical on zero apparently. Meanwhile, the probability of zero value for the HACO-OFDM signal is 0.25 instead of 0.5 for the ACO-OFDM signal, because of the signal superposition. Due to the increment for non-zero values in the PDF of the HACO-OFDM signal compared with ACO-OFDM signal, there is an increase in the average optical power of the transmitted signal.

Moreover, since the HACO and NHACO signals can be multiplexed in the time domain, the proposed method is adapted in either one or more LEDs scenario and can also be utilized with single or multiple photo-detector environments.

3. Proposed Communication System With Dimming Control

In VLC systems, the dimming control is an essential characteristic to accommodate various demands for illumination. The conventional optical OFDM schemes control the average current through the LED to adjust the luminance of LEDs, namely control the average amplitude of the transmitted

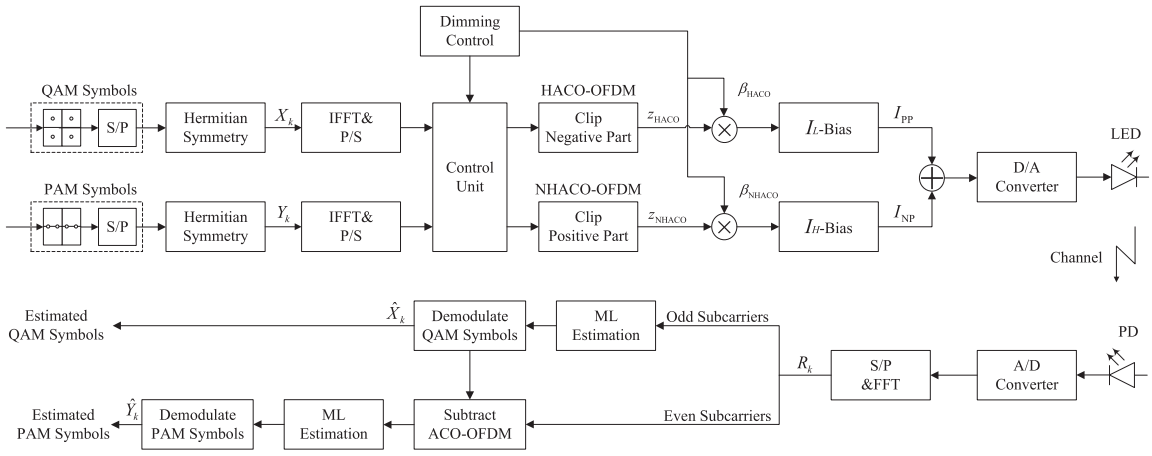

Fig. 2. Dimmable VLC transmitter and receiver based on the HACO-OFDM and NHACO-OFDM.

signals. However, the dimming control is performed by adjusting the proportion of two kinds of HACO-OFDM and NHACO-OFDM signals to obtain different average optical power in the proposed scheme.

The block diagram of the proposed dimmable VLC transmitter and receiver is illustrated in Fig. 2. The unclipped ACO-OFDM and PAM-DMT signals are firstly modulated, then the negative or positive part is clipped to generate the HACO-OFDM or NHACO-OFDM signal with a specific proportion, which is decided by the dimming control unit. The scaling factor for either HACO-OFDM or NHACO-OFDM is multiplied by the corresponding signal to achieve the required dimming level. Finally, the HACO-OFDM and NHACO-OFDM signals are mixed and fed to digital-to-analogue converter for transmission. At the receiver, the corresponding reverse operations are adopted to process the received signal.

According to the nonlinear transfer characteristic of LEDs, the transmitted signal in the time domain is limited in a restricted dynamic range [19]. Assuming I_L and I_H are correspond to the minimum and maximum allowed current values restricted by the LEDs, hence the LED dynamic range can be denoted by $I_H - I_L$, in which the transfer characteristic of LEDs is regarded as linear. In order to make sure that the transmitted signals are in the linear range, HACO-OFDM and NHACO-OFDM signals are superimposed on direct current biases and can be given by

$$I_{\mathrm{PP}} = I_L + z_{\mathrm{HACO}} \tag{16}$$

$$I_{\mathrm{NP}} = I_H + z_{\mathrm{NHACO}}, \tag{17}$$

where I_{PP} and I_{NP} are non-negative.

It should be noted that the DC bias in the proposed method is quite different compared to that in conventional DCO-OFDM. First, the DC bias in the proposed method is used to occupy the whole dynamic range of the LED, especially for the negative HACO (NHACO) signal, while the DC bias in DCO-OFDM is to ensure that the whole OFDM signal is positive, which is not efficient in terms of optical power since only half of the dynamic range is utilized. Second, for DCO-OFDM system, the DC bias is equal to the dimming level due to the symmetry property of positive and negative OFDM signal. In the proposed method, the desired dimming level is determined by the proportion of HACO-OFDM and NHACO-OFDM signals.

In the proposed dimming control approach, the I_{NP} signal is adopted for a high illumination level, while the I_{PP} is used when a low illumination level is desired. For intermediate levels, the transmitted signal is an algebraic sum of I_{PP} and I_{NP}, in which the dynamic range of LEDs can be fully exploited by both HACO-OFDM and NHACO-OFDM. Assuming the ratio of I_{NP} is α, the average amplitude

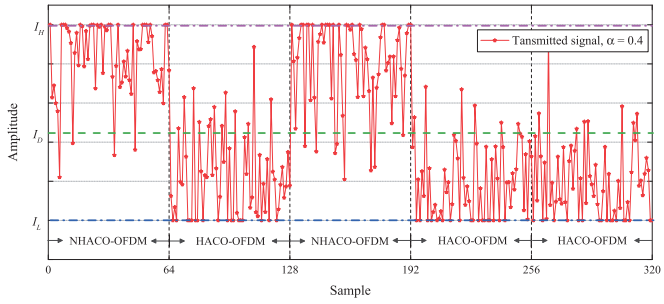

Fig. 3. Waveform of the mixed transmitted signal at $\alpha = 0.4$.

of the combined signal I_D is mathematically represented as

$$I_D = (1-\alpha)\left(I_L + \frac{\sigma_{\text{ACO}} + \sigma_{\text{PAM}}}{\sqrt{2\pi}}\right) + \alpha\left(I_H - \frac{\sigma_{\text{ACO}} + \sigma_{\text{PAM}}}{\sqrt{2\pi}}\right). \tag{18}$$

Therefore, by directly adjusting α to the required I_D, the dimming control scheme is achieved. Fig. 3 illustrates a waveform of the transmitted signal generated by HACO-OFDM and NHACO-OFDM, where the ratio α of I_{NP} is 0.4 and the number of subcarriers is set to 64. 4-QAM and 4-PAM are employed in ACO-OFDM and PAM-DMT, respectively, for both the HACO-OFDM and NHACO-OFDM systems, then the according dimming level is 44% by computation.

Moreover, the mixed transmitted signal should be further clipped when it exceeds the restricted linear range of LEDs, which leads to the clipping operation. For purpose of evaluating the undesired clipping operation of the combined signal, the scaling factors of both ACO-OFDM and PAM-DMIT are first defined as

$$\beta_{\text{ACO}} = \frac{I_H - I_L}{\sigma_{\text{ACO}}}, \quad \beta_{\text{PAM}} = \frac{I_H - I_L}{\sigma_{\text{PAM}}}. \tag{19}$$

When the scaling factors of ACO-OFDM and PAM-DMT are equal in HACO-OFDM system for simplicity, we define $\beta_{\text{HACO}} = \beta_{\text{ACO}} = \beta_{\text{PAM}}$. The scaling factors of NACO-OFDM β_{NACO}, NPAM-DMT β_{NPAM}, and NHACO-OFDM β_{NHACO} have the similar definitions.

The clipping probability of the signal is then given by

$$\begin{aligned} P\left(I_{\text{PP}} > I_H\right) &= P\left(z_{\text{HACO}} > I_H - I_L\right) = \int_{I_H - I_L}^{+\infty} f_{z_{\text{HACO}}}(z)dz \\ &= \int_{I_H - I_L}^{+\infty}\int_{-\infty}^{+\infty} f_{x_{\text{ACO}}}(I) f_{y_{\text{PAM}}}(z-I)\, dIdz \\ &= \frac{1}{2\pi\sigma_{\text{ACO}}\sigma_{\text{PAM}}}\int_{I_H - I_L}^{+\infty}\int_{0}^{z}\left(\exp\left(\frac{-I^2}{2\sigma_{\text{ACO}}^2}\right)\exp\left(\frac{-(z-I)^2}{2\sigma_{\text{PAM}}^2}\right)\right)dIdz \\ &\quad + 0.25\left[\text{erfc}\left(\frac{I_H - I_L}{\sqrt{2}\sigma_{\text{ACO}}}\right) + \text{erfc}\left(\frac{I_H - I_L}{\sqrt{2}\sigma_{\text{PAM}}}\right)\right] \end{aligned} \tag{20}$$

and

$$\begin{aligned} P(I_{\text{NP}} < I_L) &= P(z_{\text{NHACO}} < I_L - I_H) \\ &= \int_{-\infty}^{I_L - I_H} f_{z_{\text{NHACO}}}(z)dz = \int_{-\infty}^{I_L - I_H} f_{z_{\text{HACO}}}(-z)dz \\ &= \int_{I_H - I_L}^{+\infty} f_{z_{\text{HACO}}}(z)dz = P\left(I_{\text{PP}} > I_H\right). \end{aligned} \tag{21}$$

Table 1
Simulations Parameters for Dimming Control

Parameters	Value
Bandwidth	20 MHz
FFT size	512
Noise power	−10 dBm
Maximum allowed current	$I_H = 1$
Minimum allowed current	$I_L = 0$

Obviously, the clipping probability is related to the scaling factors β_{ACO} and β_{PAM}. When the scaling factors β_{ACO} and β_{PAM} are small, the probability of the clipped signal would be large, which aggravates the clipping operation. However, a large scaling factor will lead to low power efficiency of the transmitter. Therefore, a trade-off has to be made between the power efficiency and the clipping operation. In order to ensure the probability of the clipped signal less than 1%, the scaling factors β_{ACO} and β_{PAM} are set to 4 for convenience.

For the receiver, the decoding and de-multiplexing of the transmitted HACO-OFDM and NHACO-OFDM signals should also be taken into consideration. According to the property of the frequency-domain signal for NHACO-OFDM presented in (11) and (12), the decode process of the NHACO-OFDM system is the same as that of the conventional HACO-OFDM counterpart. Moreover, the bias added at the transmitter, which is sustained in one OFDM duration, only impacts on the zero subcarrier at the receiver. Therefore, based on (2) and (12), the received HACO-OFDM and NHACO-OFDM signals with DC biases can be still decoded in the same manner, and need not distinguish the HACO-OFDM and NHACO-OFDM signal at all, which leading to a simple architecture at the receiver. Compared to the conventional RPO-OFDM and AHO-OFDM schemes, the decoding of the HACO-OFDM and NHACO-OFDM should neither detect the PWM signal firstly nor require the DC bias beforehand. As a result, the de-multiplexing is not necessary for the mixed HACO-OFDM and NHACO-OFDM signals with unknown proportion and exact position at the receiver, which is an intrinsic property of the NHACO-OFDM with no penalty at all. Moreover, for determined ratio α, the multiplex mode of I_{PP} and I_{NP} at the transmitter is also flexible, since the exact positions of HACO-OFDM and NHACO-OFDM symbols have no effect on the demodulation at the receiver. Furthermore, the proposed dimming control scheme does not affect the visible light communication due to the same effective power for communication in both HACO-OFDM and NHACO-OFDM.

4. Simulation Results

Simulation results were performed to evaluate the performance of the proposed scheme. The parameters for simulation are summarized in Table 1. The total average optical power is normalized, and is divided equally between ACO-OFDM and PAM-DMT in both the HACO-OFDM and NHACO-OFDM systems to simplify the evaluation and comparison.

Fig. 4 shows the PDF of transmitted signal with different ratio α. The scaling factors are set as $\beta_{\text{HACO}} = \beta_{\text{NHACO}} = 4$. When $\alpha = 0$, the combined signal is purely HACO-OFDM modulated, while the mixed signal is totally NHACO-OFDM padded if $\alpha = 1$. It can be seen that the probability of higher amplitude value is larger, along with α increase. Hence, the different dimming levels can be achieved by adjusting with α to a proper proportion.

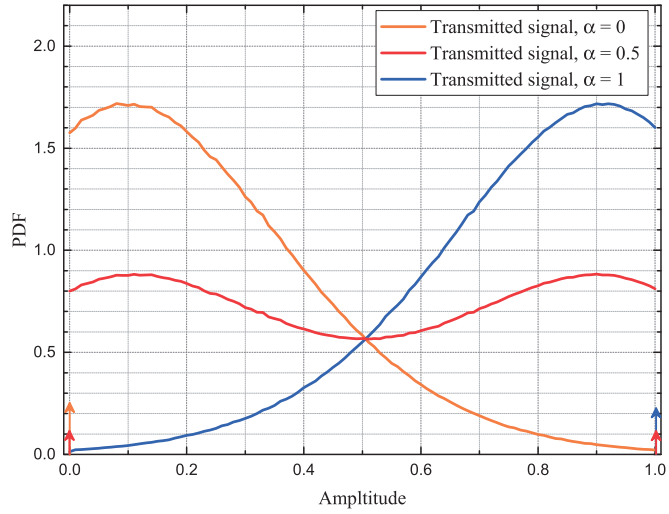

Fig. 4. PDF of the transmitted signal with different α.

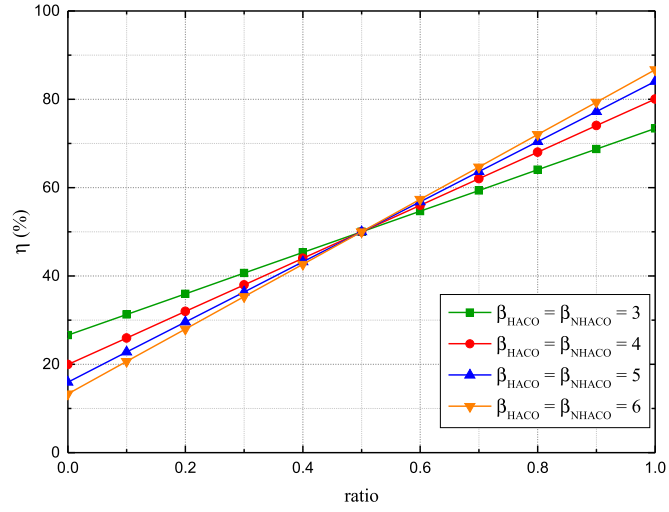

Fig. 5. Dimming level η as a function of the ratio α.

Due to illuminance is proportional to the average optical intensity, the dimming level η is defined as

$$\eta = \frac{I_D - I_L}{I_H - I_L}, \tag{22}$$

whose value is within the interval of $[0, 1]$ on account of $I_L \leq I_D \leq I_H$. Fig. 5 shows the obtained dimming level η as a function of the ratio α according to (18) and (22). It can be shown in the figure that the proposed dimming control scheme can achieve a broad dimming range. For example, the achievable dimming range is between 20% to 80% when $\beta_{\text{HACO}} = \beta_{\text{NHACO}} = 4$ are adopted. Moreover, the dimming range could be further stretched along with the increase of the scaling factors even if the desired dimming level is extremely low or high, at the cost of the power reduction of HACO-OFDM and NHACO-OFDM.

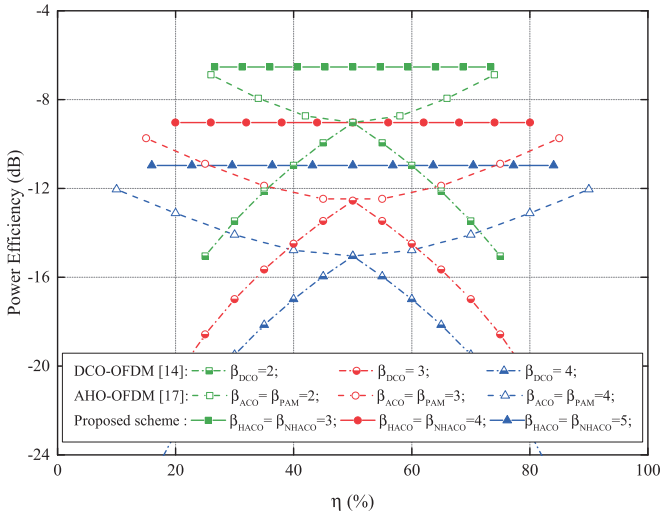

Fig. 6. Power efficiency versus different dimming level η.

In order to evaluate the power efficiency of the proposed scheme, a merit factor is defined to describe the ability to transmit effective signal as

$$\gamma = \frac{\sigma^2}{(I_H - I_L)^2} \tag{23}$$

where σ^2 denotes the power for communication. For example, in our proposed scheme, the scaling factors in both HACO-OFDM and NHACO-OFDM are fixed with equal value, therefore the powers for communication are the same and equal to $(\sigma^2_{\text{ACO}} + \sigma^2_{\text{PAM}})$ for both HACO-OFDM and NHACO-OFDM. The various proportion of two kinds of signals does not affect the power for communication, hence the merit factor of the proposed method is a constant value of $(\sigma^2_{\text{ACO}} + \sigma^2_{\text{PAM}})$. Fig. 6 illustrates the merit factor versus different dimming level η, while the y-axis is calculated in dB for clear explanation. For comparable clipping probabilities among the proposed mixed signal, AHO-OFDM [17], and DCO-OFDM [14], some cases with different scaling factors are simulated. The DC bias in both AHO-OFDM and DCO-OFDM is to ensure that the whole OFDM signal is positive, which is not efficient in terms of optical power since only part of the dynamic range is utilized. Therefore, the proposed dimming scheme has a superior power efficiency performance compared with the conventional AHO-OFDM and DCO-OFDM counterparts by exploiting the whole dynamic range of the LED.

Fig. 7 illustrates the achievable spectrum efficiency for different dimming level of the proposed method in electrical domain, where the bit error rate (BER) performance versus the normalized bit energy to noise power (E_b/N_0) is adopted for evaluation. The conventional DCO-OFDM [14], RPO-OFDM [16], and AHO-OFDM [17] are also depicted for comparisons. The extreme dimming level varies with the different scaling factors, hence different communication powers are utilized to achieve different dimming levels, which result in different E_b/N_0 at the receiver. In order to satisfy the BER requirement, different modulation schemes with various constellation orders are adopted for all kinds of achievable spectrum efficiencies. Specifically, for a target BER of 2×10^{-3} and a relative noise power of -10 dBm, the modulation orders in both ACO-OFDM and PAM-DMT for the HACO-OFDM and proposed NHACO-OFDM are adaptive to different E_b/N_0. When the dimming level is 20%, 64-QAM and 16-PAM are adopted for ACO-OFDM and PAM-DMT, respectively. Moreover, for the dimming level of 10%, the ACO-OFDM and PAM-DMT use 32-QAM and 8-PAM for modulation, respectively. Furthermore, the proposed scheme could have higher achievable spectrum efficiency compared with other counterparts due to exploiting the whole dynamic range of LED for both

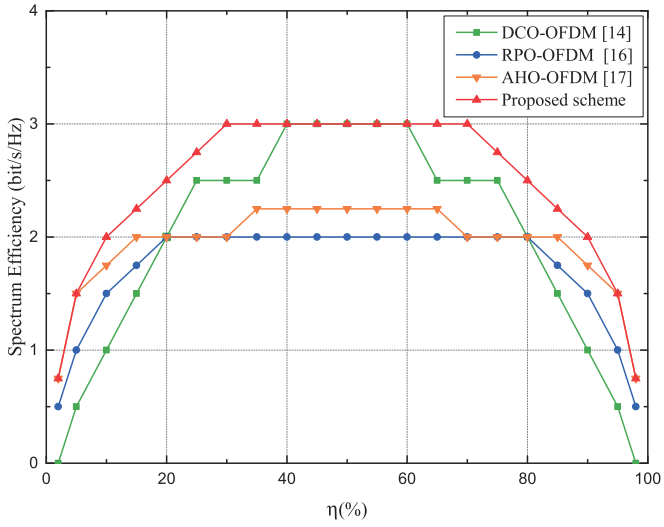

Fig. 7. Achievable spectrum efficiency for different dimming levels.

TABLE II
Simulation Results of Spectrum Efficiency

Dimming level η (%)	Proposed modulation scheme	Proposed (bit/s/Hz)	DCO-OFDM (bit/s/Hz)	RPO-OFDM (bit/s/Hz)	AHO-OFDM (bit/s/Hz)
10, 90	32-QAM, 8-PAM	2	1	1.5	1.75
20, 80	64-QAM, 16-PAM	2.5	2	2	2
30, 70	256-QAM, 16-PAM	3	2.5	2	2
40, 60	256-QAM, 16-PAM	3	3	2	2.25
50	256-QAM, 16-PAM	3	3	2	2.25

HACO-OFDM and NHACO-OFDM schemes. For example, our proposed scheme could achieve the spectrum efficiency of 2.5 bit/s/Hz when the dimming level is 20%, which is higher than other counterparts. The simulation results are also addressed in Table 2 in order to clearly compare the proposed scheme and those existing schemes.

5. Conclusion

In this paper, a dimmable illumination compatibility with communication scheme for VLC systems is proposed in this paper. By exploiting the whole dynamic range of LEDs, both the HACO-OFDM and NHACO-OFDM can achieve high power and spectrum efficeiency. After combining these two kinds of signals in proper proportion, different dimming levels can be achieved at the transmitter, while no de-multiplexing operation is needed, and the same decoding process can be adopted for HACO-OFDM and NHACO-OFDM at the receiver with the same process architecture and low complexity. Simulations have verified that the proposed method can provide a broad dimming range for illumination and achieve high-speed data transmission with higher power and spectrum efficiency compared to current existing methods.

References

[1] S. Arnon, *Visible Light Communications*. Cambridge, U.K.: Cambridge Univ. Press, 2015.
[2] A. Khalid, G. Cossu, R. Corsini, and P. Choudhury, "1-Gb/s transmission over a phosphorescent white LED by using rate-adaptive discrete multitone modulation," *IEEE Photon. J.*, vol. 4, no. 5, pp. 1465–1473, Oct. 2012.
[3] A. Jovicic, J. Li, and T. Richardson, "Visible light communication: Opportunities, challenges and the path to market," *IEEE Commun. Mag.*, vol. 51, no. 12, pp. 26–32, Dec. 2013.
[4] J. Armstrong and B. J. C. Schmidt, "Comparison of asymmetrically clipped optical OFDM and DC-biased optical OFDM in AWGN," *IEEE Commun. Lett.*, vol. 12, no. 5, pp. 343–345, May 2008.
[5] J. Armstrong and A. J. Lowery, "Power efficient optical OFDM," *Electron. Lett.*, vol. 42, no. 6, pp. 370–372, Mar. 2006.
[6] S. C. J. Lee, S. Randel, F. Breyer, and A. M. J. Koonen, "PAM-DMT for intensity-modulated and direct-detection optical communication systems," *IEEE Photon. Technol. Lett.*, vol. 21, no. 23, pp. 1749–1751, Dec. 2009.
[7] B. Ranjha and M. Kavehrad, "Hybrid asymmetrically clipped OFDM-based IM/DD optical wireless system," *J. Opt. Commun. Netw.*, vol. 6, no. 4, pp. 387–396, Apr. 2014.
[8] Q. Wang, C. Qian, X. Guo, Z. Wang, D. G. Cunningham, and I. H. White, "Layered ACO-OFDM for intensity-modulated direct-detection optical wireless transmission," *Opt. Exp.*, vol. 23, no. 9, pp. 12 382–12 393, May 2015.
[9] F. Zakar, D. Karunatilaka, and R. Parthiban, "Dimming schemes for visible light communication: The state of research," *IEEE Trans. Wireless Commun.*, vol. 22, no. 2, pp. 29–35, Apr. 2015.
[10] X. You, J. Chen, H. Zheng, and C. Yu, "Efficient data transmission using MPPM dimming control in indoor visible light communication," *IEEE Photon. J.*, vol. 7, no. 4, pp. 1–12, Aug. 2015.
[11] K. Lee and H. Park, "Modulations for visible light communications with dimming control," *IEEE Photon. Technol. Lett.*, vol. 23, no. 16, pp. 1136–1138, Aug. 2011.
[12] J. Kim and H. Park, "A coding scheme for visible light communication with wide dimming range," *IEEE Photon. Technol. Lett.*, vol. 26, no. 5, pp. 465–468, Mar. 2014.
[13] J. K. Kwon, "Inverse source coding for dimming in visible light communications using NRZ-OOK on reliable links," *IEEE Photon. Technol. Lett.*, vol. 22, no. 19, pp. 1455–1457, Oct. 2010.
[14] Z. Wang, W.-D. Zhong, C. Yu, J. Chen, C. P. S. Francois, and W. Chen, "Performance of dimming control scheme in visible light communication system," *Opt. Exp.*, vol. 20, no. 17, pp. 18 861–18 868, Aug. 2012.
[15] Y. Yang, Z. Zeng, J. Cheng, and C. Guo, "An enhanced DCO-OFDM scheme for dimming control in visible light communication systems," *IEEE Photon. J.*, vol. 8, no. 3, pp. 1–13, Jun. 2016.
[16] E. Hany and T. Little, "Reverse polarity optical-OFDM (RPO-OFDM): Dimming compatible OFDM for gigabit VLC links," *Opt. Exp.*, vol. 21, no. 20, pp. 24 288–24 299, Oct. 2013.
[17] Q. Wang, Z. Wang, and L. Dai, "Asymmetrical hybrid optical OFDM for visible light communications with dimming control," *IEEE Photon. Technol. Lett.*, vol. 27, no. 9, pp. 974–977, May 2015.
[18] D. W. Lim, S. J. Heo, and J. S. No, "An overview of peak-to-average power ratio reduction schemes for OFDM signals," *J. Commun. Netw.*, vol. 11, no. 3, pp. 229–239, Jun. 2009.
[19] H. Elgala, R. Mesleh, and H. Haas, "Non-linearity effects predistortion in optical OFDM wireless transmission using LEDs," *Int. J. Ultra Wideband Commun. Syst.*, vol. 1, no. 2, pp. 143–150, Aug. 2009.